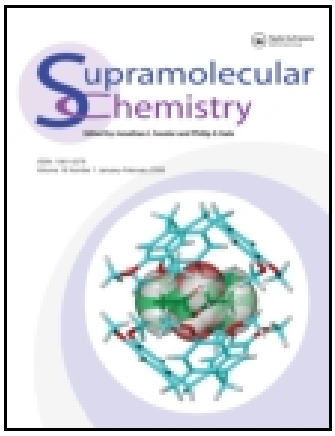

Supramolecular Chemistry
Publication details, including instructions for authors and subscription information:
http://www.tandfonline.com/loi/gsch20

Synthesis, photophysical and NMR evaluations of thiourea-based anion receptors possessing an acetamide moiety

Elaine M. Boyle [a] , Thomas McCabe [a] & Thorfinnur Gunnlaugsson [a]
[a] School of Chemistry, Trinity College Dublin, Centre for Synthesis and Chemical Biology , Dublin 2, Ireland
Published online: 31 Aug 2010.

To cite this article: Elaine M. Boyle , Thomas McCabe & Thorfinnur Gunnlaugsson (2010) Synthesis, photophysical and NMR evaluations of thiourea-based anion receptors possessing an acetamide moiety, Supramolecular Chemistry, 22:10, 586-597, DOI: 10.1080/10610278.2010.506539

To link to this article: http://dx.doi.org/10.1080/10610278.2010.506539

Supramolecular Chemistry
Vol. 22, No. 10, October 2010, 586–597

Taylor & Francis
Taylor & Francis Group

Synthesis, photophysical and NMR evaluations of thiourea-based anion receptors possessing an acetamide moiety

Elaine M. Boyle, Thomas McCabe and Thorfinnur Gunnlaugsson*

School of Chemistry, Trinity College Dublin, Centre for Synthesis and Chemical Biology, Dublin 2, Ireland

(*Received 14 April 2010; final version received 23 June 2010*)

The synthesis and photophysical evaluation of three diaryl thiourea-based anion receptors (**4**–**6**) for comparison with their urea counterparts (**1**–**3**) is outlined. These anion receptors posses an acetamide functionality on one of the aryl groups and an electron-withdrawing CF_3 group on the other. By varying the position of the acetamide group, in the *o*-, *m*- and *p*-positions of **4**–**6**, respectively, the anion binding ability was both tuneable and found to be, in some cases, significantly different from that seen for the urea analogues **1**–**3**. The binding affinities of the receptors **4**–**6**, as well as the binding stoichiometries, were evaluated using UV–vis absorption spectroscopy in MeCN. However, these receptors were not sufficiently emissive to quantify the anion recognition using fluorescence. The results confirmed strong binding of these receptors to anions such as fluoride, acetate, phosphate, pyrophosphate and chloride. Nevertheless, the overall results obtained did not conform to the anticipated trends seen for **1**–**3**, which is most likely due to the enhanced binding affinity of the thiourea analogues **4**–**6**. The binding interactions were also investigated by using ^{1}H NMR which confirmed that these receptors interacted with the anions in a stepwise manner, where the primary anion binding interaction occurred at the thiourea side, which led to an activation of the acetamide moiety towards the second anion binding interaction, an example of an allosteric activation mode.

Keywords: anions; sensing; recognition; thiourea; amide

Introduction

The recognition and sensing of anions in both organic and aqueous solutions has become an active field of research within supramolecular chemistry (*1–4*). Much effort has been devoted to the detection of anions due to the important roles they play in physiology, industry and in the environment (*5*). The recognition and sensing of anions using luminescent and colorimetric methods and, in particular, charge neutral receptors such as ureas and thioureas is of particular interest (*6–15*). Urea and thiourea groups have been widely used as anion receptor moieties as they are excellent hydrogen-bond donors (*16–24*). The anions usually form strong directional hydrogen-bonding complexes with the N—H protons, which are better hydrogen-bonding donors than simple amides; allowing the urea and thiourea moiety to be more selective in its binding (*25*). However, of these two functionalities, the thiourea is generally considered to form more stable complexes with anions than their urea counterparts, due to their enhanced N—H acidity (*21*).

The combination of either ureas or thioureas in conjunction with amides as hydrogen-bonding receptors within the same structure has only recently been explored, but this combination has given rise to significant enhancements in anion binding affinity (*26–28*). An example of such a combination are the acetamide-functionalised diaryl urea-based receptors **1**–**3**, previously synthesised within our research group (*29*), which demonstrated for the first time that the recognition and sensing of anions could occur through 'positive allosteric effects' in addition to the synergetic action of more than one hydrogen-bonding donors. These samples have an electron-withdrawing CF_3 substituent in the *para* position of one of these rings, which will make the urea moiety more electron deficient and hence, a better anion receptor. In the case of **1** and **2**, the binding of the anions at the urea moiety was shown to enhance or activate the recognition ability of the amide moiety (e.g. an allosteric effect). This enabled these receptors to bind anions in a 1:1 as well as a 1:2 binding stoichiometry; the latter occurring via the amide functional group. However, this second anion binding interaction (i.e. at the amide site) only occurred after this primary recognition at the urea site took place. The third receptor **3**, with the amide functionality *ortho* to the urea moiety, only gave rise to a 1:1 binding stoichiometry, where the amide moiety cooperatively participated in the initial anion binding event at the urea site. The receptors **1**–**3** were found to interact strongly with anions such as AcO^-, $H_2PO_4^-$, $H_2P_2O_7^{3-}$ and F^- in MeCN as determined by changes in their respective absorption spectra. Recently, Jiang and co-workers have demonstrated the use of additional functional

*Corresponding author. Email: gunnlaut@tcd.ie

ISSN 1061-0278 print/ISSN 1029-0478 online

DOI: 10.1080/10610278.2010.506539
http://www.informaworld.com

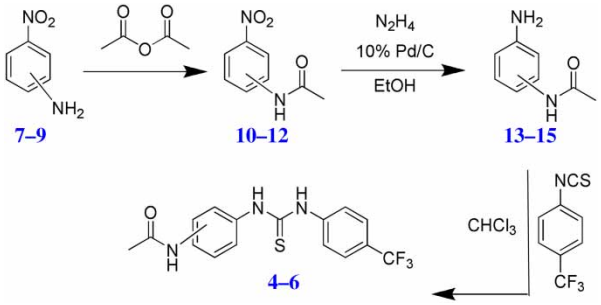

Scheme 1. Synthesis of receptors **4**, **5** and **6**.

groups to enhance the hydrogen-bonding ability of anion receptors, by developing *N*-(*o*-methoxybenzamido)-based thioureas, where the anion binding at the urea moiety was greatly enhanced by the introduction of the methoxy substituent (*30*). Based on these encouraging results, and the fact that the allosteric mode of action had not been, to the best of our knowledge, previously explored using thiourea-based anion receptors, we synthesised receptors **4**–**6**. These anion receptors are structural analogues of **1**–**3**, possessing a diaryl thiourea moiety, with the acetamide, substituent in the *para*, *meta* and *ortho* positions of **4**–**6**, respectively, and we investigated their anion binding affinity and mode of action using UV–vis absorption and ^{1}H NMR spectroscopies.

Results and discussion

Synthesis of compounds 4–6

The synthesis of compounds **4**–**6** is shown in Scheme 1. The first step was achieved by reacting the commercially available nitroaniline derivatives **7**–**9** (the *para*, *meta* and *ortho* isomers, respectively) with neat acetic anhydride overnight at room temperature to form the desired acetamide functionalities **10**–**12**, in 67, 57 and 71% yields, respectively. Subsequent reduction of the nitro group in **10**–**12** to the corresponding amine was achieved by refluxing **10**–**12** in EtOH overnight with hydrazine monohydrate ($N_2H_4{\cdot}H_2O$) in the presence of 10% Pd/C catalyst, giving rise to **13**–**15** in 73, 80 and 84% yield, respectively. Finally, the anion receptors **4**–**6** were formed by reacting **13**–**15** in $CHCl_3$ with the commercially available trifluoro-*p*-tolyl isothiocyanate at room temperature overnight under an atmosphere of argon. The resulting precipitates were collected by suction filtration and washed with cold $CHCl_3$ to give **4**–**6** in 89, 89 and 42% yield, respectively.

The three receptors were fully characterised by using ^{1}H NMR, ^{13}C NMR, mass spectrometry and elemental analysis. For instance, the ^{1}H NMR spectrum (600 MHz, DMSO-d_6) for receptor **4** showed the presence of two broad resonances, one appearing at 9.98 ppm, assigned to one of the thiourea protons, while a second resonance, appearing at 9.94 ppm, corresponded to the second thiourea proton and the amide proton, respectively. In contrast, for **5**, the thiourea protons appeared as a single broad signal at 10.06 ppm, while the amide proton resonated at 9.97 ppm. The spectrum for **6** displayed three separate resonances at 10.41, 9.74 and 9.20 ppm for the two thiourea and the amide protons, respectively. The methyl peak was observed at 2.04 ppm for **4** and **5** and at 2.08 ppm for **6**. Both the thiourea and the amide stretches were clearly distinguishable in the FTIR.

The X-ray crystal structure analysis of 6

It was found that the receptors **4**–**6**, formed crystalline material; however, of these, we were only able to obtain suitable crystals for X-ray crystallographic analysis of **6** (*31*). In the case of **6**, colourless crystals were obtained from a mixture of $CHCl_3$ and MeOH at room temperature

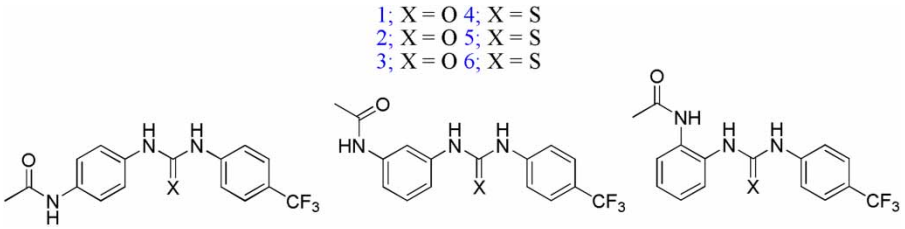

and the resulting X-ray crystal structure is shown in Figure 1(A), while Figure 1(B) demonstrates that the two aryl groups are significantly twisted out of the plane of the thiourea moiety.

The packing diagram viewed down the crystallographic *a*-axis is shown in Figure 2, illustrating an extensive intermolecular hydrogen-bonding network that exists between the amide protons and one of the NHs of the thiourea moiety; while no π–π stacking was observed for the aromatic moieties, most likely prevented by the CF_3 groups. The overall packing diagram was quite similar to that observed for **3**.

Photophysical evaluation of 4–6

The absorption spectra of **4**–**6**, when recorded at room temperature in MeCN, are shown in Figure 3. All three

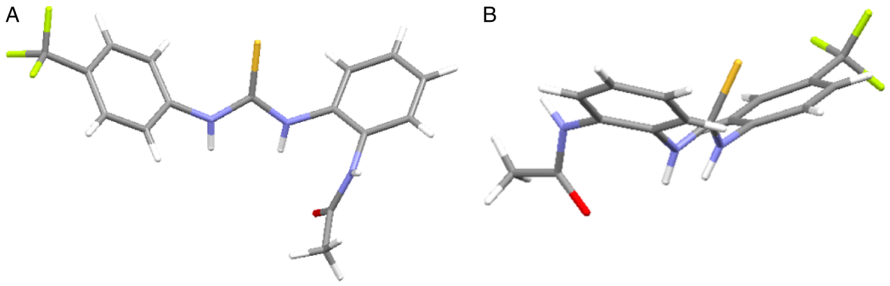

Figure 1. (A) The X-ray crystal structures of **6** showing the thiourea moiety flanked by the two aryl groups. (B) The side view, demonstrating that the two aryl groups are significantly twisted out of the thiourea plane.

receptors showed similar characteristic absorption bands centred at ca. 280–283 nm with $\varepsilon_{283} = 28{,}220\,M^{-1}\,cm^{-1}$, $\varepsilon_{282} = 19{,}220\,M^{-1}\,cm^{-1}$ and $\varepsilon_{280} = 19{,}260\,M^{-1}\,cm^{-1}$ and for **4**, **5** and **6**, respectively. A second band was also observed at ca. 248 nm for **5** and at ca. 235 nm for **6**. Upon excitation at these λ_{max}, the receptors only gave rise to weak fluorescence emission. Hence, the anion recognition was only monitored by observing the changes in the ground state of **4**–**6**.

Anion binding evaluations of compounds 4–6

The anion binding ability of receptors **4**–**6**, as well as the stoichiometries for the resulting binding interactions, was investigated by titrations of a stock solution of the receptor (ca. 1×10^{-5} M) with various anion solutions in MeCN at room temperature. The anions studied were dihydrogen phosphate ($H_2PO_4^-$), acetate (AcO^-), hydrogenpyrophosphate ($HP_2O_7^{3-}$), fluoride (F^-) and chloride (Cl^-) as their tetrabutylammonium (TBA) salts. The absorption spectra of **4**, upon titration with the various anions, all exhibited a bathochromic shift upon binding to these anions. The spectral data obtained from the titration of **4** with AcO^- are presented in Figure 4(A).

Figure 4(A) shows that the band centred at ca. 283 nm was shifted to ca. 294 nm with the formation of a 'pseudo isosbestic point' at ca. 282 nm. It can be seen from Figure 4(B) that the number of equivalents of anion required to reach a plateau is approximately 2 with only minor changes occurring thereafter (e.g. 2–5 equiv.). The same behaviour was observed for $HP_2O_7^{3-}$ and F^-, indicating the rapid formation of a very stable host–guest species in solution. In the case of $H_2PO_4^-$, the band centred at ca. 283 nm exhibited a slightly smaller red shift of ca. 7 nm with the plateau being reached upon ca. 15 equiv. of anion. The spectral changes observed for Cl^-, were, however, less significant and occurred only at relatively higher

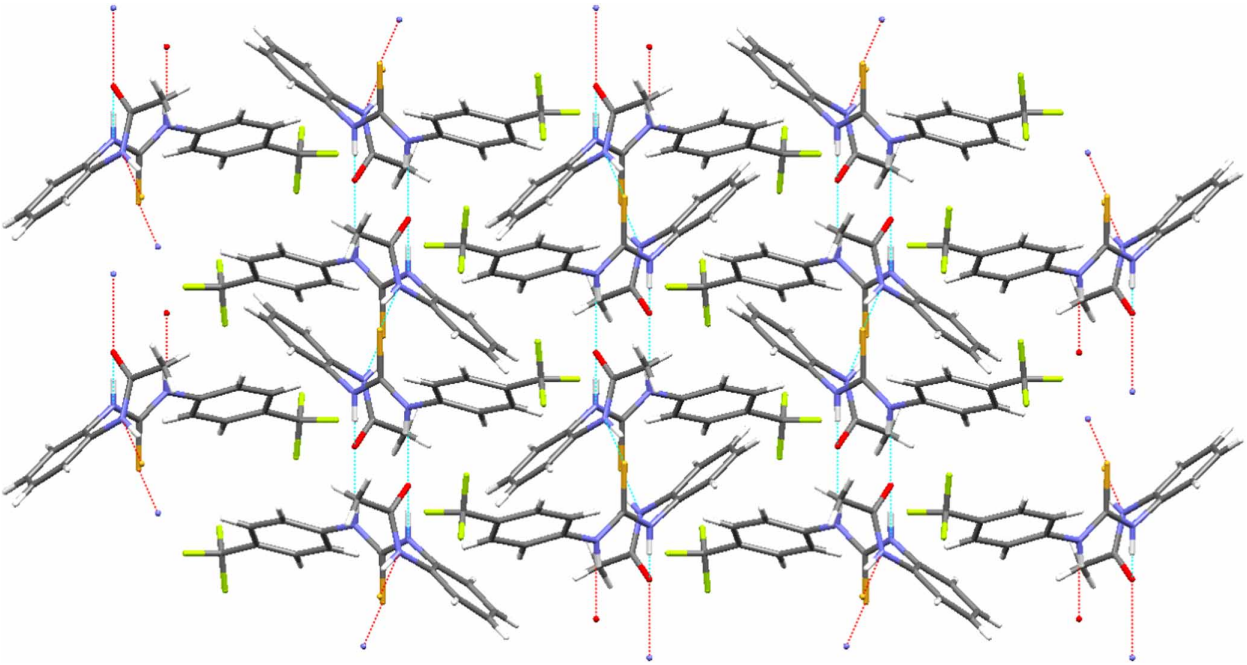

Figure 2. Packing diagram of **6** viewed down the crystallographic *a*-axis.

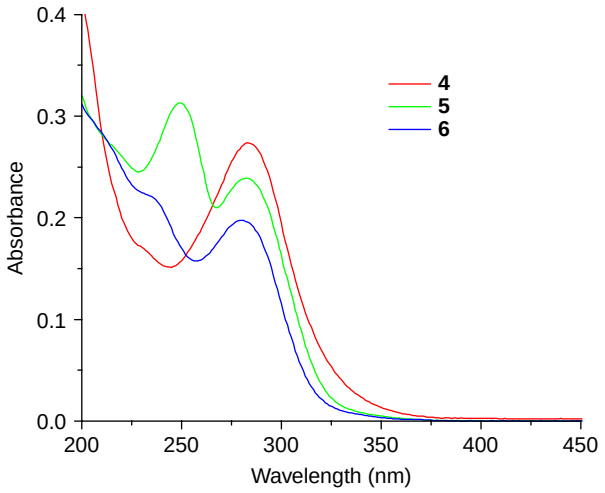

Figure 3. The absorption spectra of receptors **4**–**6** in MeCN (ca. 1×10^{-5} M).

concentrations of the anion, indicating a weaker binding interaction in comparison to the above anions.

From the changes observed, binding constants ($\log K$) for complex formation between the anions (**G**) and **4** (**L**) were determined by fitting the absorption data using the non-linear least-squares regression program SPECFIT™. The obtained stoichiometries and corresponding $\log K$ values are listed in Table 1.

The first binding mode was ascribed to the interaction between the anions and the thiourea moiety of **4** through H-bonding. Upon further addition of the anion, a second binding interaction was observed. This interaction was attributed to the anion binding to the amide functionality *para* to the urea moiety. When the results of **4** were compared to the corresponding urea receptor **1**, it was found that the binding affinity of **4** with the various anions was generally stronger, which is the anticipated trend, as discussed above. For example, AcO^- and $H_2PO_4^-$ gave rise to binding constants of $\log K_{1:1} = 6.31$ (± 0.17) and $\log K_{1:1} = 5.34$ (± 0.24), respectively, for receptor **4**, while the binding constants for the urea analogue **1** were determined to be $\log K_{1:1} = 5.29$ (± 0.03) and $\log K_{1:1} = 4.93$ (± 0.05) for these anions, respectively. It is also worth noting that the presence of two **G:L** complexes, namely the 1:1 and 2:1 species between **4** and Cl^-, were found to exist while the urea receptor **1** only formed a 1:1 complex. This is most likely due to the enhanced acidity of the thiourea receptor in comparison to the urea analogue.

Having established the anion binding ability of **4**, the structural isomer **5** was next investigated. Besides the characteristic absorption band $\lambda_{max} = 282$ nm, receptor **5** also had a band centred at ca. 252 nm. The largest spectral changes observed were those between **5** and $HP_2O_7^{3-}$, as illustrated in Figure 5(A).

It can be seen from Figure 5(A) that the absorption spectrum of **5** was red-shifted from ca. 282 nm to ca. 287 nm with the concomitant loss of the band centred at ca. 252 nm at higher concentrations of the anion; while Figure 5(B) indicates that a plateau was reached before the addition of 5 equiv. of the anion (insert is the result of the full titration).

Similar behaviour was also observed upon addition of anions such as $H_2PO_4^-$, F^- and AcO^-. The spectral changes observed for Cl^- again occurred only at higher concentrations, and the bathochromic shift caused by the interaction with Cl^- was the smallest among the anions studied. The observed changes strongly indicate that the interaction between **5** and the various anions is due to H-bonding. By fitting the changes for each titration, the binding constants for these anions and **5** were determined using SPECFIT™, the results of which are shown in Table 2.

It can be seen that the changes observed for each anion were best fitted to 1:1 and 2:1 stoichiometries. It appeared that the formation of the 1:1 species was the most dominant species in solution for AcO^- and Cl^-, with a much smaller contribution from the 2:1 stoichiometry at higher equivalent of the anion, as shown in Figure 6.

The results obtained for **5** were significantly different than those observed for its urea counterpart **2**. The binding constants determined for **2** and anions such as F^-, $H_2PO_4^-$ and $HP_2O_7^{3-}$ were all best fitted to 1:1, 1:2 and 2:1 stoichiometries with the anion becoming 'sandwiched' between the urea moieties of the two ligands before the activation of the acetamide functionality led to the formation of the 2:1 species. This behaviour was not observed between **5** and any of the anions studied. It was also noted that while AcO^- gave rise to slightly higher 1:1 binding to **5** ($\log K_{1:1} = 5.61$ (± 0.11)) than to **2** ($\log K_{1:1} = 5.41$ (± 0.02)), Cl^- gave a lower binding constant of $\log K_{1:1} = 3.69$ (± 0.05) and $\log K_{1:1} = 4.86$ (± 0.09) for **5** and **2**, respectively.

The third receptor **6**, with the acetamide functionality in the *ortho* position, was studied in the same manner as above. This analogue showed the most interesting results as it was anticipated that only a 1:1 species between the host and anion would be formed, as only this receptor offers the possibility of direct cooperative binding between the amide and the thiourea functionality, as was previously observed with the urea analogue **3**. However, analysis of the data obtained, as shown in Table 3, indicated that this was not the case. Indeed, the changes observed for all of the anions were best fitted to both 1:1 and 2:1 stoichiometries. This is most likely due to the enhanced anion binding ability of the thiourea moiety.

The titration of **6** with $H_2PO_4^-$ is shown in Figure 7(A). The band centred at ca. 280 nm was shifted to ca. 290 nm (with the formation of an isosbestic point at ca. 235 nm). As can be seen from Figure 7(B), an excellent fit was obtained for the changes observed in Figure 7(A).

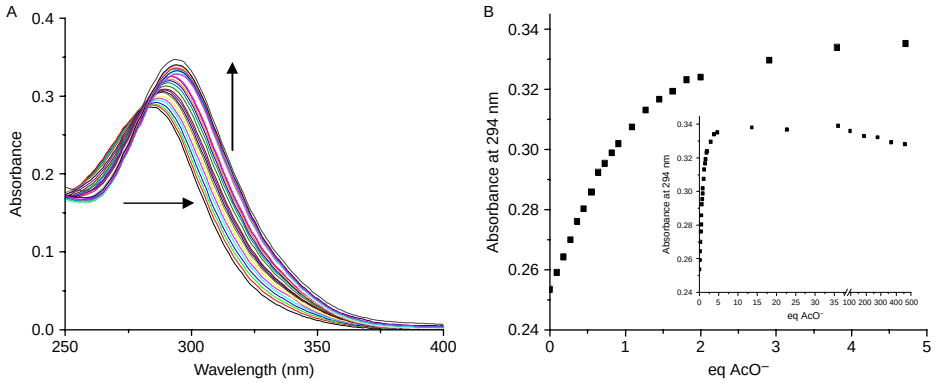

Figure 4. (A) Changes observed in the absorption spectra of **4** (8.98×10^{-6} M) upon titration with AcO^- (0–4.67 mM) in MeCN. (B) The changes in the absorbance at 294 nm as a function of equivalents of AcO^-. The inset shows the changes observed between 0 and 500 equiv. of AcO^-.

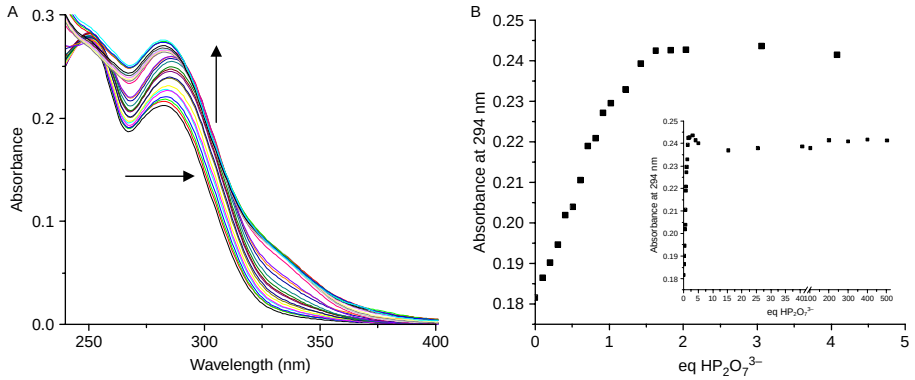

Figure 5. (A) Changes in the absorption spectra of **5** (1.1×10^{-5} M) upon titration with $HP_2O_7^{3-}$ (0–4.58 mM) in MeCN. (B) The changes in the absorbance at 294 nm as a function of equivalents of $HP_2O_7^{3-}$. The inset shows the changes observed between 0 and 500 equiv. of $HP_2O_7^{3-}$.

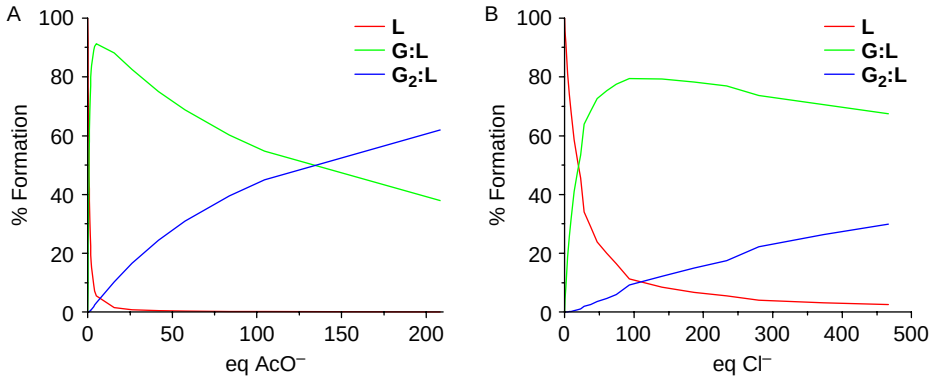

Figure 6. (A) Speciation distribution diagram for the absorption titration of **5** (**L**) with AcO^-. (B) Speciation distribution diagram for the absorption titration of **5** (**L**) with Cl^-.

From these changes two binding constants were determined, where the 1:1 stoichiometry resulted in a $\log K_{1:1} = 4.81$ (± 0.01) and a second strong binding interaction with a $\log K_{2:1} = 4.60$ (± 0.14) was also determined. Both AcO^- and F^- exhibited a strong 1:1 binding interaction, with $\log K_{1:1} = 5.46$ (± 0.05) and $\log K_{1:1} = 5.30$ (± 0.05), respectively. The binding interaction for the 2:1 species for these anions was not as strong

Table 1. Binding constants and binding modes between anions and receptor **4**.

	Binding mode G_n:L_m	log $K_{n:m}$	Standard deviation (±)
AcO^-	**G:L**	6.31	0.17
	G_2:L	5.12	0.37
F^-	**G:L**	4.84	0.1
	G_2:L	4.3	0.28
$H_2PO_4^-$	**G:L**	5.34	0.24
	G_2:L	4.66	0.46
$HP_2O_7^{3-}$	**G:L**	5.76	0.007
	G_2:L	1.52	0.13
Cl^-	**G:L**	4.1	0.13
	G_2:L	3.26	0.31

Table 2. Binding constants and binding modes between anions and receptor **5**.

Anion (G)	**Binding** mode **G_n**:L_m	**log** $K_{n:m}$	**Standard deviation** (±)
AcO^-	G:L	5.61	±0.11
	G_2:L	2.93	±0.23
F^-	G:L	5.39	±0.07
	G_2:L	3.71	±0.25
$H_2PO_4^-$	G:L	4.42	±0.19
	G_2:L	4.945	±0.39
$HP_2O_7^{3-}$	G:L	5.46	±0.15
	G_2:L	2.77	±0.30
Cl^-	G:L	3.69	±0.05
	G_2:L	1.90	–[a]

[a] Value fixed, as the affinity is low.

as that seen for $H_2PO_4^-$, as illustrated in Figure 8. Once again, the smallest spectral changes observed were for Cl^-, where the 280 nm band was red-shifted by only 5 nm.

When these results were compared to that of urea receptor **3**, some similarities were found. For instance, the binding constants obtained for AcO^- are almost identical with $\log K_{1:1} = 5.45$ (±0.02) and $\log K_{1:1} = 5.46$ (±0.02) for **3** and **6**, respectively. The results for Cl^- are also comparable with $\log K_{1:1} = 3.60$ (±0.05) and $\log K_{1:1} = 3.20$ (±0.07) for **3** and **6**, respectively. This pattern is repeated with the other anions studied. However, the main anomaly is the 2:1 stoichiometries obtained for **6** with all of the anions investigated. This is in stark contrast with the results obtained for the urea analogue **3** as it appears that the amide functionality of receptor **3** is orientated such that a 2:1 species is possible.

Table 3. Binding constants and binding modes between anions and receptor **6**.

Anion (G)	**Binding mode G_n:L_m**	**log $K_{n:m}$**	**Standard deviation (±)**
AcO^-	**G:L**	5.46	±0.05
	G_2:L	3.44	±0.28
F^-	**G:L**	5.30	±0.05
	G_2:L	3.47	±0.21
$H_2PO_4^-$	**G:L**	4.81	±0.01
	G_2:L	4.60	±0.14
$HP_2O_7^{3-}$	**G:L**	6.33	±0.06
	G_2:L	2.13	±0.19
Cl^-	**G:L**	3.20	±0.07
	G_2:L	2.0	±0.01

In summary, the interaction between the three receptors **4**–**6** and various anions was investigated using UV–vis absorption spectroscopy. Receptor **4** was found to generally bind to the anions more strongly than its urea counterpart **1**, as anticipated. Receptor **5** was found to interact with the anions in a different manner to its urea analogue **2**, with the changes observed for each anion best fitted to 1:1 and 2:1 stoichiometries while receptor **2** was also found to bind the anions in a 1:2 stoichiometry by

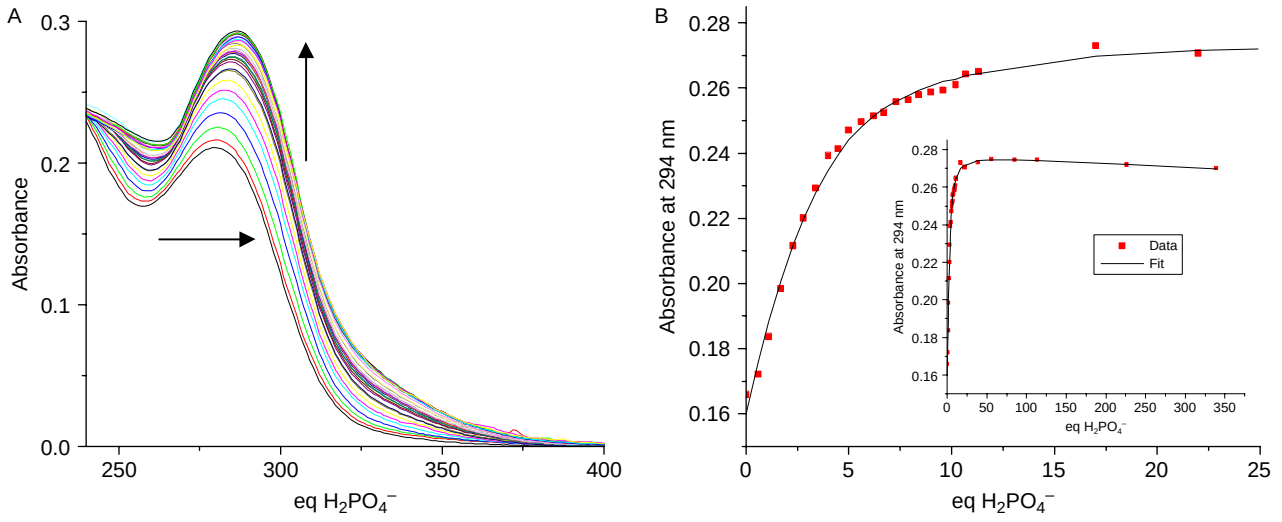

Figure 7. (A) Changes in the absorption spectra of **6** (1.09×10^{-5} M) upon titration with $H_2PO_4^-$ (0–4.72 mM) in MeCN. (B) Fit to the experimental binding isotherm obtained using SPECFIT™. The inset shows the fit between 0 and 350 equiv. of $H_2PO_4^-$.

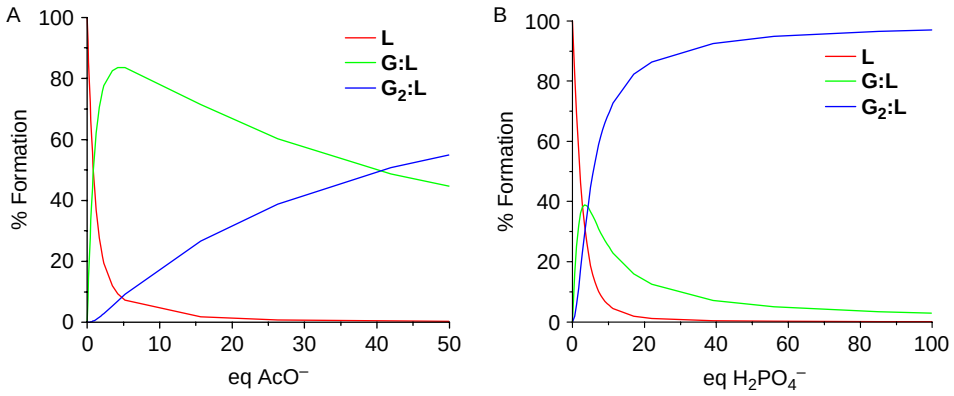

Figure 8. (A) Speciation distribution diagram for the absorption titration of **6** (**L**) with AcO^-. (B) Speciation distribution diagram for the absorption titration of **6** (**L**) with $H_2PO_4^-$.

sandwiching the anion between two urea moieties. Finally, receptor **6** was shown to have the acetamide functionality free to bind the anions in a 2:1 stoichiometry, while it is cooperatively involved in binding with the urea moiety of receptor **3**. With the view of further analysing the binding interactions of these thiourea derivatives with the above anions, we next carried out ^{1}H NMR titrations.

^{1}H NMR analysis of 4–6 on the binding of various anions

^{1}H NMR spectroscopy is a useful technique to directly observe the effect of anion complexation on the NH protons of sensors such as **4**–**6**. The ^{1}H NMR titrations of **4**–**6** were all carried out in DMSO-d_6, which enabled us to clearly follow the changes in the chemical environment of all of the N—Hs in these structures upon binding to the anions. The stack plot of the ^{1}H NMR spectra of **4** upon addition of various equivalents of Cl^- is shown in Figure 9, which clearly demonstrates the dramatic changes observed in the structure of **4** upon anion recognition. It can be seen that the thiourea protons experience a significant downfield shift upon binding to Cl^-, and interestingly, the thiourea protons become two separate resonances upon addition of Cl^-. The amide proton also experiences a shift, however this is less significant, and in contrast, only minor changes were observed for the aromatic protons.

The changes in the thiourea and amide resonances ($\Delta\delta$) were plotted against the equivalents of anion added, shown in Figure 10(A) and (B), respectively. The thiourea protons are shifted downfield, with changes still occurring even at higher concentrations of Cl^-. The amide proton is also immediately shifted downfield with the more significant changes occurring after ca. 2 equiv. These results confirm the results previously observed from the absorption studies.

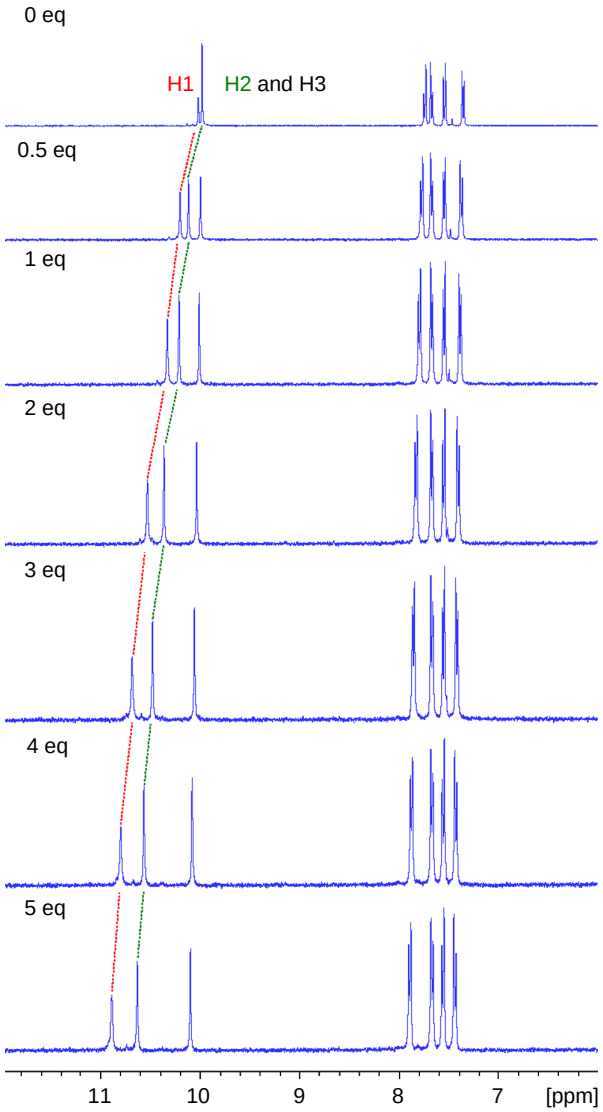

Figure 9. Stack plot of the ^{1}H NMR (400 MHz, DMSO-d_6) spectra of **4** upon addition of 0.5, 1, 2, 3, 4 and 5 equiv. of Cl^-. H1 and H2 are the thiourea protons, while H3 is the amide NH.

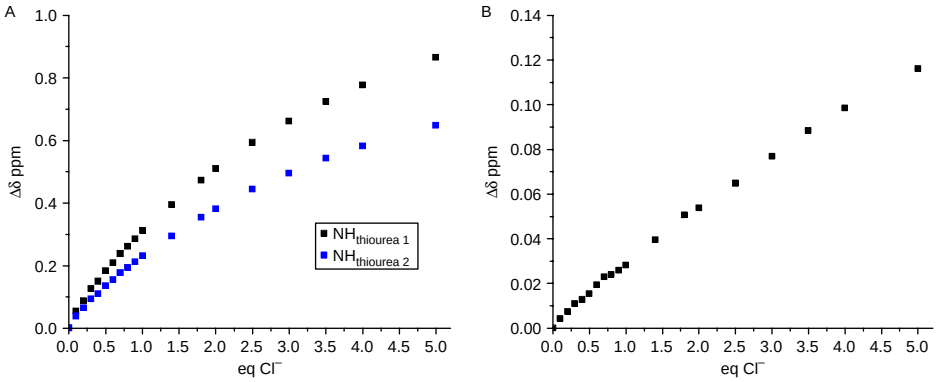

Figure 10. (A) Changes in the H1 resonance of **4** (as $\Delta\delta$) upon titration with Cl^-. Similar changes were seen for the H2 proton. (B) Changes seen for the H3 resonance during the same titration.

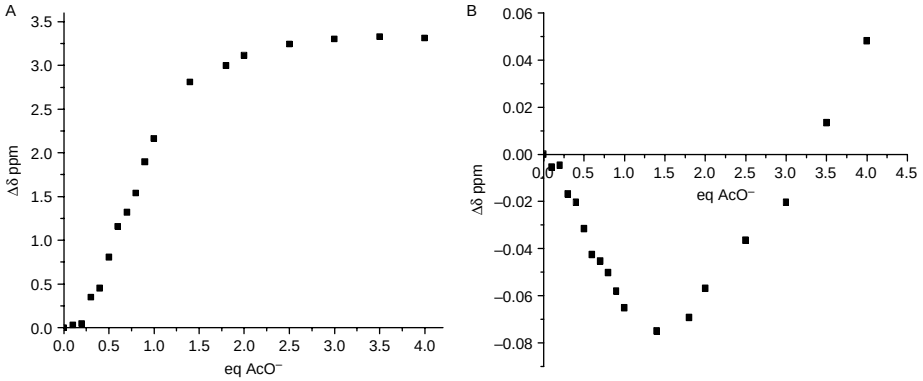

Figure 11. (A) Changes in the H1 resonance of **4** (as $\Delta\delta$) upon titration with AcO^-. (B) Changes seen for the H3 resonance during the same titration.

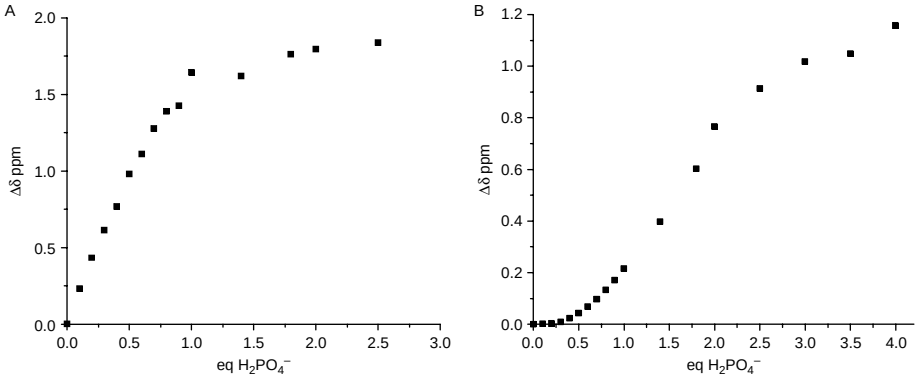

Figure 12. (A) Changes in the H1 resonance of **5** (as $\Delta\delta$) upon titration with $H_2PO_4^-$. (B) Changes seen for the H3 resonance during the same titration.

The results observed between **4** and AcO^-, illustrated in Figure 11(A), show that the binding of the anion had a major effect on the N—H protons, which in the case of the thiourea N—Hs occurred within the addition of 0–1.5 equiv. of AcO^-. It can be seen from Figure 11(B) that the amide proton is shifted upfield initially. However, beyond 1.5 equiv. is shifted downfield as a function of an increased AcO^- concentration. This phenomenon was also observed for the urea analogues **1**–**3**, and was attributed to the anion initially binding at the urea moiety via H-bonding with the amide functionality becoming activated at higher concentrations of the anion. These results also correlate with the

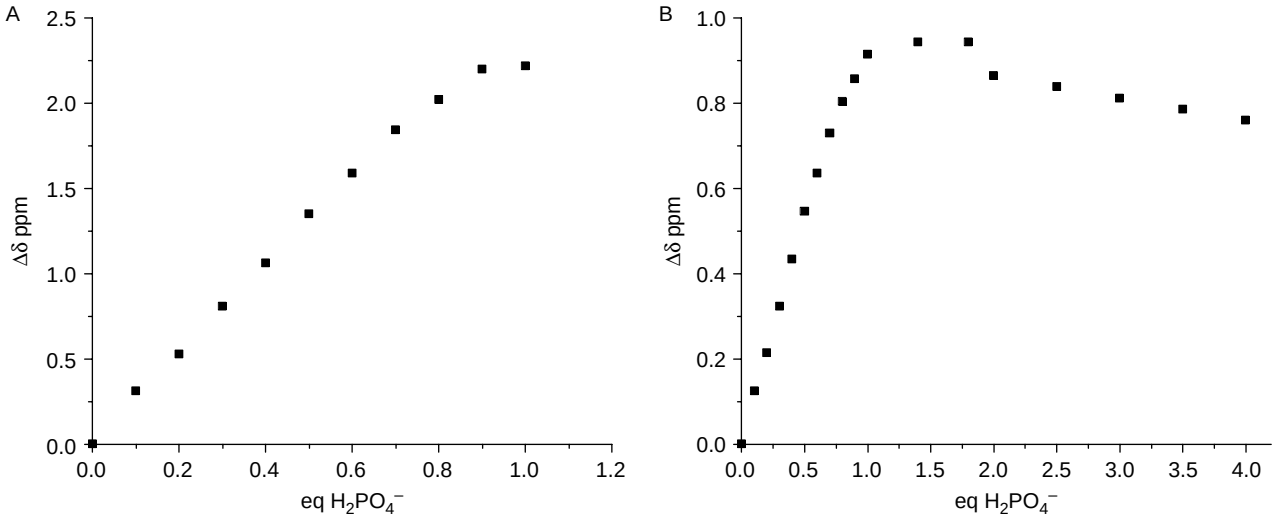

Figure 13. (A) Changes in the H1 resonance of **6** (as $\Delta\delta$) upon titration with $H_2PO_4^-$. (B) Changes seen for the H3 resonance during the same titration.

absorption studies carried out with **4**–**6** and the various anions discussed above.

The changes observed in the N—H protons of receptor **5** when titrated with $H_2PO_4^-$ are shown in Figure 12. It can be seen that the thiourea protons, Figure 12(A), experience the majority of the changes between 0 and 1 equiv. However, the amide proton, Figure 12(B), continues to experience a shift even at higher concentrations of the anion, indicating a second binding event. Again, these results confirm the results previously determined from the absorption studies.

Similar results were seen for the titration between **5** and AcO^-, with the majority of the changes occurring between 0 and 1.5 equiv. for the thiourea protons. The amide proton was again initially shifted upfield but at higher concentrations of the anion it experienced a downfield shift.

The third receptor, **6** which demonstrated the most unusual results in the absorption studies out of the three receptors, was also investigated by ^{1}H NMR. The interaction with this receptor with the various anions was indeed quite strong. In general, the thiourea protons experienced a large downfield shift with a concomitant broadening of the two resonances. For example, Figure 13(A) shows the plot of the changes in the thiourea resonance ($\Delta\delta$) against the equivalents of $H_2PO_4^-$ added. Even at lower concentrations of the anion, the protons were so broadly shifted that the resonances were not visible. However, it appeared that a plateau was beginning to form at ca. 1 equiv. of $H_2PO_4^-$. The amide proton was therefore the only resonance which could be followed, Figure 13(B).

Similar changes were seen between **6** and AcO^- and $HP_2O_7^{3-}$. In contrast, the results seen for the Cl^- titration were slightly less significant, leading to only small broadening of the thiourea protons. Figure 14 shows the stack plot of the ^{1}H NMR spectra of **6** upon addition of various equivalents of Cl^-, and also demonstrated that significantly more pronounced changes were observed in the aromatic region of **6** upon binding to this anion.

Receptors **4**–**6** also showed significant shifts when titrated with F^-. The thiourea protons of all three receptors showed a broadening of the resonances, making it difficult to track the changes. At higher concentrations, deprotonation of the thiourea protons occurred, signified by the appearance of a triplet at ca. 16 ppm. However, the amide proton was clearly visible even at higher concentrations of F^-. Figure 15 shows the plot of the changes in the amide resonances of **4** and **5** ($\Delta\delta$) against the equivalents of F^- added.

The amide proton was found to experience an upfield shift until ca. 2 equiv. of F^- after which it shifted downfield. It was also at this point that the appearance of the HF_2^- triplet at ca. 16 ppm appeared, a clear indication of a deprotonation event (*24*).

These ^{1}H NMR studies are in agreement with the data obtained from the UV–vis absorption titrations. It was found that the position of the acetamide functionality on the ring greatly influenced the anion binding affinity of receptors **4**–**6**, especially for receptor **6** where it is available as a second binding site for the various anions but is unavailable to bind them in the urea analogue **3**. This second binding event is a direct consequence of the thiourea moiety present in receptor **6**.

Conclusion

In conclusion, three novel anion receptors **4**–**6** have been synthesised and fully characterised, and their various spectroscopic properties analysed in the presence of

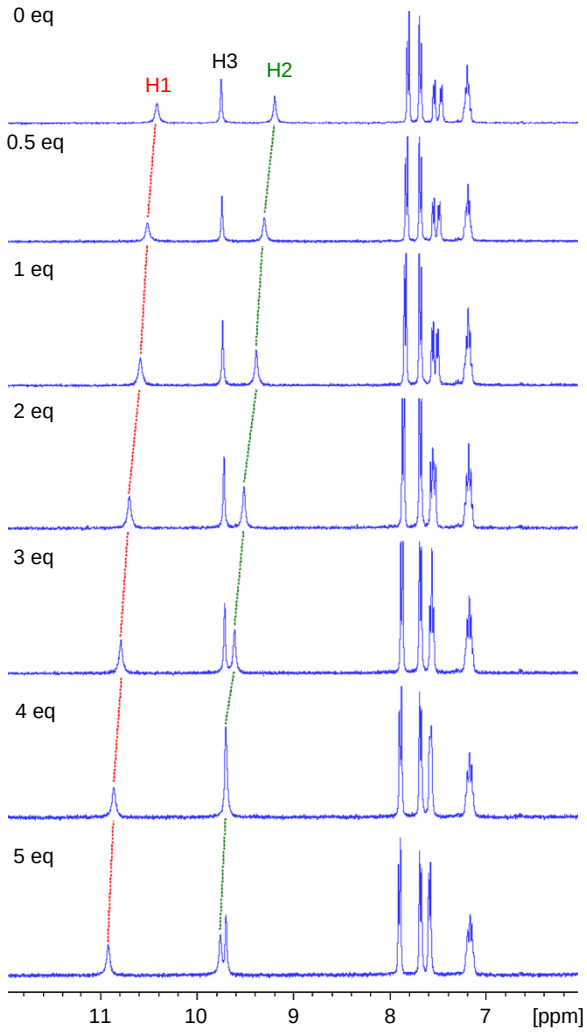

Figure 14. Stack plot of the ^{1}H NMR (400 MHz, DMSO-d_6) spectra of **6** upon addition of 0.5, 1, 2, 3, 4 and 5 equiv. of Cl^-. H1 and H2 are thiourea protons, while H3 is the amide NH.

several biologically important anions. All of the receptors were found to interact via H-bonding with anions such as AcO^-, F^-, $H_2PO_4^-$, $HP_2O_7^{3-}$ and Cl^- as determined by the changes in their respective absorption spectra. A possible conformation for the hydrogen-bonding complex formed between **4**–**6** and AcO^- is illustrated in Figure 16.

When compared to their urea counterparts, **1**–**3**, many of the anticipated trends were not observed. For example, it was expected that the thiourea receptors would show increased binding affinity to the various anions compared to the urea analogues, however in some instances this was not found to be the case. Also, receptor **3** was only expected to bind in a 1:1 stoichiometry due to cooperative binding between the amide and thiourea functionalities, but all of the anions formed a 2:1 species with this receptor. It has been suggested that thioureas are conformationally more flexible than their urea analogues, leading to the possibility that any conformational changes within the thiourea receptors may affect, to a certain extent, their anion binding properties (*32*). We have also compared the binding affinity of **4** and **5** in particularly with that of **1** and **2**, respectively. These demonstrate that the thiourea receptors are in general stronger anion binders. We have also compared the ratio between $\log K_{1:1}$ and $\log K_{2:1}$ (as $\log K_{2:1}/\log K_{1:1}$) for these receptors. These results show that for **4**, the binding of AcO^-, F^-, $H_2PO_4^-$ and Cl^- gave $\log K_1/\log K_2$ values of 0.71, 0.83, 0.87 and 0.79 for these anions, respectively, while for the urea analogue **1**, this ratio was 0.66, 0.51, 0.62 and 0.58. Similar trends were also seen for **5** upon comparison with **2**. This seems to suggest that the 'allosteric effect' might be stronger in the thiourea systems. We are currently investigating this allosteric phenomenon further.

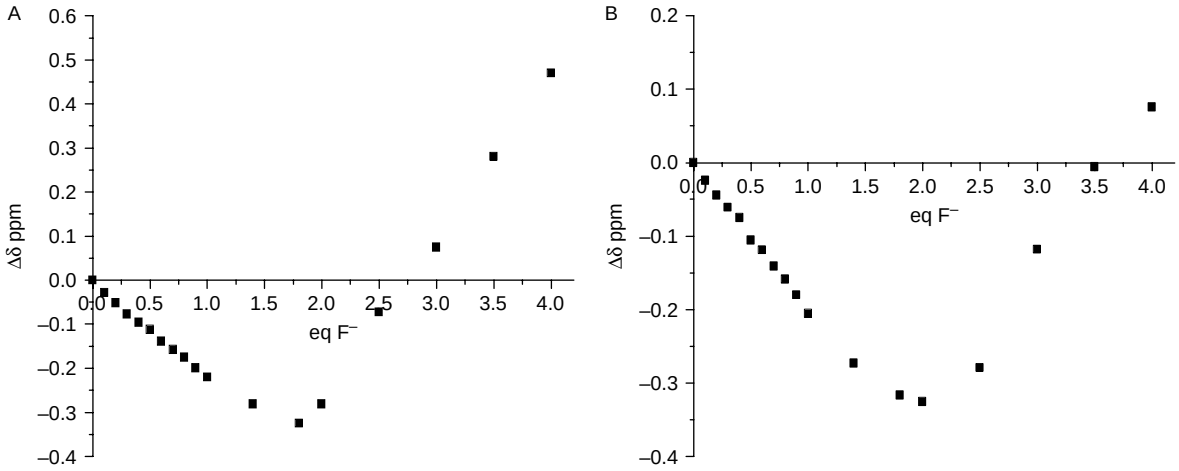

Figure 15. (A) Changes in the H3 resonance of **4** (as $\Delta\delta$) upon titration with F^-. (B) Changes seen for the H3 resonance of **5** upon titration with F^-.

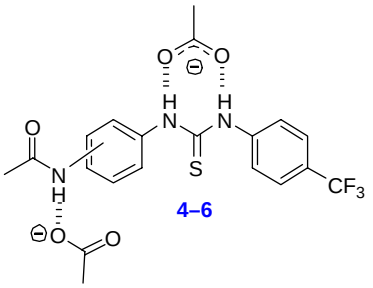

Figure 16. Possible hydrogen-bonding complex between **4**–**6** and AcO^-.

Experimental

General

Reagents (obtained from Sigma-Aldrich Ireland Ltd.) and solvents were purified using standard techniques. Melting points were determined using a GallenKamp melting point apparatus. Infrared spectra were recorded on a Mattson Genesis II FTIR spectrophotometer equipped with a Gateway 2000 4DX2-66 workstation. ^{1}H NMR spectra were recorded at 400 MHz using a Bruker Spectrospin DPX-400 instrument. ^{13}C NMR spectra were recorded at 100 MHz using a Bruker Spectrospin DPX-400 instrument.

Spectroscopic studies

All measurements were made at room temperature. UV–vis absorption spectra were recorded using a Varian Cary 50 spectrophotometer. The solvents used were of HPLC grade. The wavelength range was 200–600 nm with a scan rate of 600 nm min^{-1}. The blank used was a sample of the solvent system the titration was undertaken in. Baseline correction measurements were used in all spectra. All stock solutions were prepared freshly before measurement. Data analysis was conducted using Origin 7.5® and SPECFIT™. The effect of anions on the sensors was investigated by the addition of different volumes of an anion ($H_2PO_4^-$, AcO^-, $HP_2O_7^{3-}$, F^-, Cl^-) solution in MeCN, with different concentrations (5×10^{-3}–0.1 M), to a 2.7 ml solution of **4**–**6** in MeCN. In each case, additions were accompanied with magnetic stirring. All titrations were repeated twice to ensure reproducibility. All the anions were used in the form of their TBA salts, $(C_4H_9)_4N^+$. These salts were purchased from Aldrich and used without further purification.

NMR titrations

The experiments were carried out by using a known amount of the host dissolved in 0.6 ml of solvent ([host] $\approx 7.4 \times 10^{-3}$ M). The anion guest solutions were prepared such that 2 μl of the solution would give 0.1 equiv. of anion ([anion] $\approx 0.22 \times 10^{-1}$ M). After each addition of the anion guest to the NMR tubes, the ^{1}H NMR spectra were recorded (400 MHz) after 5 min equilibration.

Synthesis

General experimental procedure for compounds 4–6

The relevant amino acetamide (**13**–**15**) (1 equiv.) was placed in a 50 ml round bottom flask and dissolved with $CHCl_3$. Trifluoro-*p*-tolyl isocyanate (1.1 equiv.) was added, and the solution was then stirred at room temperature overnight under an argon atmosphere. The resulting precipitate was filtered and washed with cold $CHCl_3$. The obtained solid was then dried under vacuum followed by crystallisation.

N-(4-(3-(4-(Trifluoromethyl)phenyl)thioureido) phenyl)acetamide (4)

Receptor **4** was synthesised according to the above procedure using *N*-(4-aminophenyl)-acetamide **(13)** (0.28 g, 1.89 mmol) and trifluoro-*p*-tolyl isothiocyanate (0.57 g, 2.83 mmol). The resulting precipitate was then filtered and washed with cold $CHCl_3$ to yield the pure compound as an off white solid (0.59 g, 89% yield). Mp 209–211°C. Calculated for $C_{16}H_{14}N_3OF_3S{\cdot}0.05CHCl_3$: C, 53.50; H, 3.93; N, 11.65%. Found C, 53.34; H, 3.79; N, 11.64%; HR-MS (*m*/*z*) (ES^+) calculated for $C_{16}H_{13}N_3OF_3S$ $m/z = 352.0731$ $[M - H]^-$. Found $m/z = 352.0731$; ^{1}H NMR (600 MHz, d_6-$(CD_3)_2SO$) δ_H: 9.98 (br s, 1H, $NH_{thiourea}$), 9.94 (br s, 1H, $NH_{thiourea+amide}$), 7.76 (d, 2H, Ar-H, $J = 8.5$ Hz), 7.68 (d, 2H, Ar-H, $J = 8.5$ Hz), 7.56 (d, 2H, Ar-H, $J = 8.5$ Hz), 7.37 (d, 2H, Ar-H, $J = 8.5$ Hz), 2.04 (s, 3H, CH_3); ^{13}C NMR (150 MHz, d_6-$(CD_3)_2SO$) δ_C: 179.5, 168.0, 143.4, 136.3, 133.9, 125.5 (q, $J_{13C-19F} = 4$ Hz), 125.3 (q, $J_{13C-19F} = 26$ Hz), 125.2, 124.5, 124.3 (q, $J_{13C-19F} = 270$ Hz), 122.7, 119.0, 23.8; IR ν_{max} (cm^{-1}) 3302, 3206, 3094, 1669, 1618, 1599, 1567, 1521, 1330, 1304, 1158, 1130, 1112, 1072, 1014, 839, 404.

N-(3-(3-(4-(Trifluoromethyl)phenyl)thioureido) phenyl)acetamide (5)

Receptor **5** was synthesised according to the above procedure using *N*-(3-aminophenyl)-acetamide **(14)** (0.16 g, 1.08 mmol) and trifluoro-*p*-tolyl isothiocyanate (0.33 g, 1.63 mmol). The resulting precipitate was then filtered and washed with cold $CHCl_3$ to yield the pure compound as an off white solid (0.34 g, 89% yield). Mp 169–171°C. Found $m/z = 352.0707$; calculated for $C_{16}H_{14}N_3OF_3S{\cdot}0.05CHCl_3$: C, 53.64; H, 3.94; N, 11.69%. Found C, 53.76; H, 3.87; N, 11.59%; HR-MS (*m*/*z*) (ES^+) calculated for $C_{16}H_{14}N_3OF_3SNa$ $m/z = 376.0731$ $[M + Na]^+$; ^{1}H NMR (600 MHz, d_6-$(CD_3)_2SO$) δ_H: 10.06 (s, 2H, $NH_{thiourea}$), 9.97 (s, 1H, $NH_{acetamide}$), 7.77 (d, 2H, Ar-H, $J = 8.2$ Hz), 7.76 (dd, 1H, Ar-H, $J = 2.0$ Hz, 2.0 Hz), 7.68 (d, 2H, Ar-H, $J = 8.2$ Hz), 7.37 (dd, 1H, Ar-H, $J = 8.0$ Hz, 2 Hz), 7.25 (t, 1H, Ar-H, $J = 8.0$ Hz), 7.20 (dd, 1H, Ar-H_6, $J = 8.0$ Hz, 2.0 Hz), 2.04

(s, 3H, CH_3); ^{13}C NMR (150 MHz, d_6-$(CD_3)_2SO$) δ_C: 179.4, 168.3, 143.4, 139.6, 139.3, 128.7, 125.5 (q, $J_{13C-19F} = 4$ Hz), 124.4 (q, $J_{13C-19F} = 272$ Hz), 123.8 (q, $J_{13C-19F} = 32$ Hz), 122.8, 118.2, 115.4, 114.1, 23.9; IR ν_{max} (cm^{-1}) 3320, 3232, 3180, 3126, 3064, 1654, 1597, 1573, 1545, 1453, 1417, 1320, 1305, 1288, 1254, 1161, 1104, 1063, 1016, 840, 785, 713, 680.

*N-(2-(3-(4-(Trifluoromethyl)phenyl)thioureido) phenyl)acetamide (**6**)*

Receptor **6** was synthesised according to the above procedure using *N*-(2-aminophenyl)-acetamide **(15)** (0.14 g, 0.92 mmol) and trifluoro-*p*-tolyl isothiocyanate (0.28 g, 1.38 mmol). The resulting precipitate was then filtered and washed with cold $CHCl_3$ to yield the pure compound as an off white solid (0.14 g, 42% yield). Mp 179–182°C. Found $m/z = 352.0707$; calculated for $C_{16}H_{14}N_3OF_3S{\cdot}0.04CHCl_3$: C, 53.79; H, 3.95; N, 11.73%. Found C, 53.81; H, 3.99; N, 11.60%; HRMS (m/z) (ES^+) calculated for $C_{16}H_{14}N_3OF_3SNa$ $m/z = 376.0700$ $[M + Na]^+$; ^1H NMR (600 MHz, d_6-$(CD_3)_2SO$) δ_H: 10.41 (br s, 1H, $NH_{thiourea}$), 9.74 (s, 1H, NH_{amide}), 9.20 (br s, 1H, $NH_{thiourea}$), 7.82 (d, 2H, Ar-H, $J = 8.5$ Hz), 7.69 (d, 2H, Ar-H, $J = 8.5$ Hz), 7.55 (d, 1H, Ar-H, $J = 7.1$ Hz), 7.47 (d, 1H, Ar-H, $J = 7.1$ Hz), 7.21 (t, 1H, Ar-H, $J = 7.1$ Hz), 7.18 (t, 1H, Ar-H, $J = 7.1$ Hz), 2.08 (s, 3H, CH_3); ^{13}C NMR (150 MHz, d_6-$(CD_3)_2SO$) δ_C: 180.1, 169.1, 143.3, 132.6, 132.0, 128.2, 126.1 (q, $J_{13C-19F} = 4$ Hz), 125.7, 125.6 125.5 (q, $J_{13C-19F} = 272$ Hz), 124.8, 124.4 (q, $J_{13C-19F} = 272$ Hz), 122.7, 23.4; IR ν_{max} (cm^{-1}) 3197, 3110, 3012, 1642, 1598, 1537, 1500, 1481, 1442, 1319, 1296, 1260, 1239, 1166, 1156, 1106, 1064, 1016, 845, 762, 736, 700.

Acknowledgements

We thank Trinity College Dublin, Science Foundation Ireland (SFI RFP 2008 grant), and PRTLI Cycle 4 (CSCB funding) for financial support, and Drs Steve Comby and Emma Veale for their help and suggestions.

References

(1) Gunnlaugsson, T.; Glynn, M.; Tocci (née Hussey), G.M.; Kruger, P.E.; Pfeffer, F.M. *Coord. Chem. Rev.* **2006**, *250*, 3094–3317.
(2) Gale, P.A.; Garcia-Garrido, S.E.; Garric, J. *Chem. Soc. Rev.* **2008**, *37*, 151–190.
(3) Steed, J.W. *Chem. Commun.* **2006**, 2637–2649.
(4) Caltagirone, C.; Gale, P.A. *Chem. Soc. Rev.* **2009**, *38*, 520–563.
(5) Sessler, J.L.; Gale, P.A.; Cho, W.S. *Anion Receptor Chemistry*; Royal Society of Chemistry: Cambridge, UK, 2006.
(6) Ali, H.D.P.; Quinn, S.J.; McCabe, T.; Kruger, P.E.; Gunnlaugsson, T. *New J. Chem.* **2009**, *33*, 793–800.
(7) Gunnlaugsson, T.; Ali, H.D.P.; Glynn, M.; Kruger, P.E.; Hussey, G.M.; Pfeffer, F.M.; dos Santos, C.M.G.; Tierney, J. *J. Fluoresc.* **2005**, *15*, 287–299.
(8) Veale, E.B.; Gunnlaugsson, T. *J. Org. Chem.* **2008**, *73*, 8073–8076.
(9) Veale, E.B.; Tocci, G.M.; Pfeffer, F.M.; Kruger, P.E.; Gunnlaugsson, T. *Org. Biomol. Chem.* **2009**, *7*, 3447–3454.
(10) Quinlan, E.; Matthews, S.E.; Gunnlaugsson, T. *J. Org. Chem.* **2007**, *72*, 7497–7503.
(11) Ali, H.D.P.; Kruger, P.E.; Gunnlaugsson, T. *New J. Chem.* **2008**, *32*, 1153–1161.
(12) Pfeffer, F.M.; Kruger, P.E.; Gunnlaugsson, T. *Org. Biomol. Chem.* **2007**, *5*, 1894–1902.
(13) Duke, R.M.; Gunnlaugsson, T. *Tetrahedron Lett.* **2007**, *48*, 8043–8047.
(14) dos Santos, C.M.G.; McCabe, T.; Gunnlaugsson, T. *Tetrahedron Lett.* **2007**, *48*, 3135–3139.
(15) dos Santos, C.M.G.; Glynn, M.; McCabe, T.; de Melo, J.S.S; Burrows, H.D.; Gunnlaugsson, T. *Supramol. Chem.* **2008**, *20*, 407–418.
(16) Gunnlaugsson, T.; Davis, A.P.; Glynn, M. *Chem. Commun.* **2001**, 2556–2557.
(17) Lowe, A.J.; Dyson, G.A.; Pfeffer, F.M. *Org. Biomol. Chem.* **2007**, *5*, 1343–1346.
(18) Pfeffer, F.M.; Lim, K.F.; Sedgwick, K.J. *Org. Biomol. Chem.* **2007**, *5*, 1795–1799.
(19) Quinlan, E.; Matthews, S.E.; Gunnlaugsson, T. *Tetrahedron Lett.* **2006**, *47*, 9333–9338.
(20) Palacios, M.A.; Nishiyabu, R.; Marquez, M.; Anzenbacher, P., Jr. *J. Am. Chem. Soc.* **2007**, *129*, 7538–7544.
(21) Gomez, D.E.; Fabbrizzi, L.; Licchelli, M.; Monzani, E. *Org. Biomol. Chem.* **2005**, *3*, 1495–1500.
(22) Pfeffer, F.M.; Buschgens, A.M.; Barnett, N.W.; Gunnlaugsson, T.; Kruger, P.E. *Tetrahedron Lett.* **2005**, *46*, 6579–6584.
(23) Pfeffer, F.M.; Gunnlaugsson, T.; Jensen, P.; Kruger, P.E. *Org. Lett.* **2005**, *7*, 5357–5360.
(24) Gunnlaugsson, T.; Kruger, P.E.; Lee, T.C.; Parkesh, R.; Pfeffer, F.M.; Hussey, G.M. *Tetrahedron Lett.* **2003**, *44*, 6575–6578.
(25) Gunnlaugsson, T.; Davis, A.P.; Hussey, G.M.; Tierney, J.; Glynn, M. *Org. Biomol. Chem.* **2004**, *2*, 1856–1863.
(26) Brooks, S.J.; Gale, P.A.; Light, M.E. *Chem. Commun.* **2006**, *41*, 4344–4346.
(27) Kang, J.; Lee, Y.J.; Lee, S.K.; Lee, J.H.; Park, J.J.; Kim, Y.; Kim, S.-J.; Kim, C. *Supramol. Chem.* **2010**, *22*, 267–273.
(28) Wu, F.-Y.; Li, Z.; Guo, L.; Wang, X.; Lin, M.-H.; Zhao, Y.-F.; Jiang, Y.-B. *Org. Biomol. Chem.* **2006**, *4*, 624–630.
(29) dos Santos, C.M.G.; McCabe, T.; Watson, G.W.; Kruger, P.E.; Gunnlaugsson, T. *J. Org. Chem.* **2008**, *73*, 9235–9244.
(30) Jiang, Q.-Q.; Darhkijav, B.; Liu, H.; Wang, F.; Li, Z.; Jiang, Y.-B. *Chem. Asian J.* **2010**, *5*, 543–549.
(31) CCDC number 771081. Software Reference Manual, version 5.625; Bruker Analytical X-Ray Systems Inc. Madison, WI, Sheldrick, G.M. SHELXTL, An Integrated System for Data Collection, Processing, Structure Solution and Refinement, Bruker Analytical X-Ray Systems Inc., Madison, WI, 2001.
(32) (a) Culstelcean, R.; Engle, N.L.; Bonnesen, P.V. *CrystEngComm.* **2007**, *9*, 452–455. (b) Custelcean R. *Chem. Commun.* **2008**, 295.